IEEE Access
Multidisciplinary | Rapid Review | Open Access Journal

Received 27 April 2023, accepted 7 May 2023, date of publication 16 May 2023, date of current version 1 June 2023.

Digital Object Identifier 10.1109/ACCESS.2023.3276787

RESEARCH ARTICLE

Voltage and Reactive Power Regulation With Synchronverter-Based Control of PV-STATCOM

AJINKYA J. SONAWANE, (Student Member, IEEE), AND AMOD C. UMARIKAR, (Member, IEEE)
Discipline of Electrical Engineering, Indian Institute of Technology at Indore, Indore 453552, India
Corresponding author: Amod C. Umarikar (amodu@iiti.ac.in)

This work was supported by the Department of Science and Technology Fund for Improvement of Science and Technology Infrastructure (DST FIST) Program under Grant SR/FST/ETI-400.

ABSTRACT This paper presents a synchronverter based photovoltaic (PV) system as STATCOM (PV-STATCOM), in which inverter exchanges active and reactive power with the grid. The proposed system provides reactive power compensation during daytime as well as nighttime. Additional operating modes for PV-STATCOM are proposed to enhance its capability. The proposed controller is compared with conventional control based PV-STATCOM on the basis of its performance with different tests. The key difference between conventional control and synchronverter is that synchronverter emulates inertia to control the frequency and voltage of the system. It is observed that the proposed system reduces frequency deviation and provides satisfactory regulation of the point of common coupling (PCC) voltage during full STATCOM mode and partial STATCOM mode. The low voltage ride through (LVRT) test is also performed on the proposed system. In the weak grid situation, the proposed PV-STATCOM performs in a more stable manner than the conventional PV-STATCOM in both reactive power and PCC voltage control mode. The study is performed on EMTDC/PSCAD simulation software. Real Time Control Hardware In Loop (CHIL) test is performed on Real Time Digital Simulator (RTDS) with a microcontroller to validate the proposed controller strategy and control design.

INDEX TERMS PV-based synchronverter, grid-connected inverter, synchronverter, PV-STATCOM, STATCOM, virtual synchronous generator.

NOMENCLATURE

List of Abbreviations

PV	Photovoltaic.
PCC	Point of common coupling.
LVRT	Low voltage ride through.
CHIL	Controller-Hardware-In-Loop.
RTDS	Real-Time-Digital-Simulator.
STATCOM	Static synchronous compensator.
VSC	voltage source compensator.
VSG	Virtual Synchronous Generator.
DG	Distribution generator.
MPPT	Maximum power point tracking.
DSP	Digital signal processor.
SCR	Short circuit ratio.

List of Symbols

V_{dc}	Dc-link voltage [V].
I_{dc}	Dc input current to the VSC [A].
C_{dc}	Dc-link capacitance [μf].
i_{sd}	d-axis output current of VSC [A].
i_{sq}	q-axis output current of VSC [A].
L_f	Inductance of filter [mH].
R_f	Internal resistance of L_f [Ω].
C_f	Filter capacitor [μf].
R_d	Damping resistance in series with C_f [Ω].
L_t	Leakage inductance of the interface transformer [mH].
P_{pv}	Output power of PV array [W].
P_s	Output active power of the inverter [W].
P_{cdc}	Power stored in a dc-link capacitor [W].
V_{pcc}	Voltage amplitude of PCC voltage [V].
Q_s	Output reactive power of the inverter [VAR].

The associate editor coordinating the review of this manuscript and approving it for publication was Ahmed F. Zobaa.

This work is licensed under a Creative Commons Attribution-NonCommercial-NoDerivatives 4.0 License.
For more information, see https://creativecommons.org/licenses/by-nc-nd/4.0/

$\beta_1, \beta_2, \beta_3$ Gains of DC-link controller.
K_{pvc}, K_{ivc} PI gains PCC voltage controller.

I. INTRODUCTION

The voltage related issues occur in the power system due to sudden changes in load, system faults, etc. Use of synchronous machines as synchronous condensers to improve the power system voltage profile is well known. A synchronous condenser has stable operating characteristics but leads to losses [1]. A STATic synchronous COMpensator (STATCOM) has been proposed as a viable option to increase the power transfer capacity [2]. STATCOM is a voltage source converter (VSC) based compensator, which achieves its objectives by absorbing and releasing a reactive power. STATCOM is used to regulate PCC voltage and enhance stability of the power system [2].

STATCOM has a similar structure/characteristics to PV system connected to the grid. Following to this, a concept of PV-STATCOM is proposed in [3] and [4] to increase solar PV farm utilization in the daytime and nighttime. In [5] and [6], the utilization of PV-STATCOM was validated for increasing the connectivity of neighboring wind farm. A novel damping controller is proposed in [7] to damp power oscillation to enhance system capacity for PV-STATCOM. The PV-STATCOM as a smart inverter is demonstrated in [8] and the control design for the smart inverter is validated on Real Time Digital Simulator (RTDS). In [9], the PV-STATCOM on the field and effectiveness of PV-STATCOM control to stabilize a critical induction motor is demonstrated. A frequency control is also proposed with a conventional current control technique in PV-STATCOM [10]. However, the use of this frequency controller increases the controller order, which may increase the complexity. The voltage control ability with the PV system is given in [11] and [12]. Various aspects of PV-STATCOM are presented in [13], and discuss about advantages of using PV-STSTCOM in solar farm.

Generally, two important tasks of STATCOM are voltage control and reactive power control [14]. In reactive power control, output of the STATCOM always follows the reference; however, the reactive power is automatically adjusted to follow the voltage reference in voltage control mode. Different inverter topologies for STATCOM are proposed in [15]. Various controller techniques of STATCOM are suggested to fulfil various objectives [16]- [17]. The virtual synchronous generator (VSG), i.e., virtual inertia based controller strategies for STATCOM, are proposed in [18], [19], and [20]. These controller mimics the behavior of a synchronous machine and extracts all the advantage of it. Also, inertia is provided for reactive compensation and makes the STATCOM behave like a synchronous condenser. The controller benefit is that by controlling inertia, the system's dynamic performance is improved and reduces the impact of power and voltage fluctuation due to grid and DGs power injection. Synchronverter is one of the virtual synchronous machine controller techniques proposed in [21]. A PV based synchronverter is investigated in [22] and studies stability analysis of the system with different PV mode of operation. The synchronverter as a STATCOM proposed in [18] demonstrates the operation with reactive power control and PCC voltage control. The S-STATCOM is proposed in [19] and discusses the voltage imbalance compensation capability. The synchronverter based STATCOM control technique proposed in [18] and [19] cannot share the reactive power in voltage control mode while operating in parallel. The stability analysis of synchronverter as a STATCOM is studied in [20] and demonstartes the improvement of dynamic stability of system. In [23] the case study on the exchange of reactive power with synchronverter is performed on a benchmark system. Other virtual inertia based controller strategies for STATCOM are proposed in [24], [25], and [26]. The VSCOM is proposed in [24], which adjusts the inertia by using a proportional integrator (PI) controller for reactive power loop and achieves fast response by increasing the dc-link controller's response speed to avoid oscillation due to lower value of dc-link capacitor. Reference [24] outlines that in the weak grid, VSCOM is more stable than the traditional control. A virtual inertia based compensator is proposed in [25], where inertia is built in dc-link voltage controller with the inner current control loop. Using current control, a virtual inertia based PV-STATCOM is discussed in [26]; however, it did not discuss controls for reactive power compensation and different PV-STATCOM operating modes. From this survey, it can be noticed that the synchronverter based PV-STATCOM is yet to be investigated. Also, synchronverter based STATCOM study with different control mode is yet to be carried. The benefits of synchronverter providing short term frequency control during transients without losing the ability to control reactive power when operating as PV-STATCOM is missing in the literature. Understandably the STATCOM has similar characteristics to PV plant connected to the grid via VSC. To explore the possibility of the application of a synchronverter as STATCOM in the PV system to enhance power system stability, it is necessary to investigate synchronverter as a PV-STATCOM.

This paper investigates and validates the synchronverter based PV-STATCOM for the control of reactive power and point of common coupling (PCC) voltage. The small-signal model of the study system is used to design the controller parameters and their response at a different controller parameter value. In addition to this, the proposed system is tested on different PV-STATCOM operating modes. A new MPP and nonMPP based operating modes for synchronverter based PV-STATCOM are investigated. The performance of conventional PV-STATCOM and synchronverter based PV-STATCOM is analyzed. It is observed that in case of a weak grid the proposed PV-STATCOM is more stable and overcomes the limitations of typical PV-STATCOM. Also, the benefits of synchronverter providing short term frequency control during transients without losing the ability to control reactive power is achieved. The study is performed by using EMTDC/PSCAD simulation software. Further, Real Time

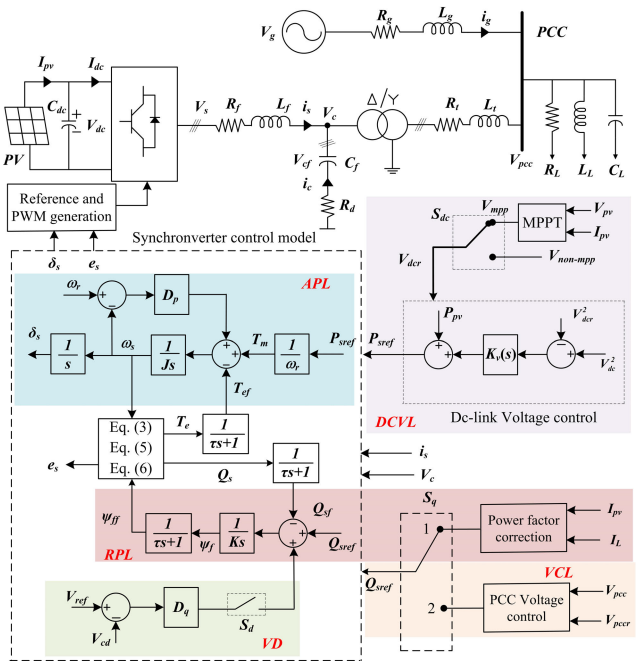

FIGURE 1. Diagram of synchronverter based PV-STATCOM.

CHIL test is performed on RTDS with a microcontroller to validate the proposed controller strategy and control design.

The paper structure is as follows. Section II discusses the concept of PV-STATCOM. System configuration is given in section III. The modeling and control design procedure for the system is described in section IV. The proposed system is validated through simulation in section V and laboratory results in section VI. Section VII concludes the paper.

II. SYSTEM CONFIGURATION

A. STUDY SYSTEM

Fig. 1 shows a diagram of the study system. A 10 KVA distributed generation (DG) is tied to the grid using Δ-Y coupling transformer. A 400V V_{L-L} distribution system equivalent model with line impedance R_g and L_g is connected to a PCC. RLC load (R_L, L_L and C_L, respectively) is also connected at the PCC. The load is supplied by both the grid and DG. Photovoltaic (PV) source is used as a DG source. The voltage at maximum power point is 800V at which output power is 10kW which is maximum PV power output. A PV source interface with the grid using a two-level six pulse IGBT-based VSC. To reduce harmonics generated due to VSC LCL filter is used. R_f represents losses due to the internal resistance of filter inductor L_f and on-state resistance of IGBT, while L_f is the filter inductor. R_d is damping resistance connected in series with filter capacitance C_f. C_f is chosen to limit reactive power exchange is not more than 5 % of rated power. R_t and L_t are the resistance and leakage inductance of the transformer, respectively. The incremental conductance technique is used in this article to achieve maximum power point [27]. This system is controlled by various controllers like synchronverter control, MPPT control, PCC voltage control and dc-link voltage control so that the PV system can operate as PV-STATCOM and in various operating modes as per the system requirement.

B. GENERAL OPERATING MODES OF PV-STATCOM

The PV system generates real power for 8-9 hours and it is at its peak for 3-4 hours in 24 hours. Except for these peak hours, the VSC operates less than its capacity and the unutilized capacity of VSC is used to exchange the reactive power. Real power generation is the priority in the whole system operation. Three modes of PV-STATCOM are full PV mode, full STATCOM mode and partial STATCOM mode. The partial STATCOM mode is applicable in the daytime, where the inverter's remaining capacity is utilized to exchange reactive power after real power transfer. The full STATCOM mode is applicable in the nighttime as the rea1 power generation is zero. The PV generation is discontinued by either increasing voltage across the PV panel to open-circuit voltage or disconnecting PV Panels. In this mode, full priority is given to the reactive power exchange. Sometimes in case of a critical need for reactive power exchange, the full STATCOM mode also applicable in the daytime to maintain the PCC voltage after disconnecting the real power generation. The system returns to its previous mode once the requirement of the grid is fulfilled. In full PV mode, the full capacity of VSC is used to transfer the real power.

III. PV-STATCOM CONTROL SCHEME

The complete controller structure for PV-STATCOM is shown in Fig. 1 and as given in Table 2. The control scheme has different control loops, which are discussed below:

APL (Active power loop): It regulates the active power and keeps the system synchronized with the grid.

DCVL (Dc-link voltage control loop): It controls the dc-link voltage by controlling the output power of the inverter. The reference for dc-link voltage is generated based on the MPP or nonMPP mode.

RPL (Reactive power loop): It controls the output reactive power of the inverter.

VCL (Voltage control loop): It regulates the PCC bus voltage.

VDL (Voltage droop loop): It provides the feature of voltage droop operating mode with both reactive power and PCC voltage control mode.

Synchronverter based STATCOM [18], operates in either reactive power mode, PCC voltage control mode or voltage droop mode. The proposed control scheme provides the different operating modes. In one of the mode, the PCC voltage controller maintains PCC voltage while the voltage droop control is active at the same time. This may give an advantage in parallel operation of multiple inverters.

The different operating modes can be achieved based on the combination of states of the switches shown in Fig. 1. States of switches S_d and S_q decide four operating modes: reactive power mode (Q mode), PCC voltage control mode (V mode),

TABLE 1. PV-STATCOM operating modes.

S_q	S_d	S_{dc}	Operating Mode
1	OFF	1 or 2	Q mode
2	OFF	1 or 2	V mode
1	ON	1 or 2	VD mode
2	ON	1 or 2	V mode + VD mode
1 or 2	OFF or ON	1	MPP mode
1 or 2	OFF or ON	2	nonMPP mode

voltage droop control mode (VD mode) and PCC voltage plus voltage droop control mode. PCC voltage plus voltage droop control mode can allow parallel operation of several inverter. Switch S_{dc} decides whether the PV system is functioning in MPP mode or nonMPP mode. The different controllers are explained in the following subsections.

A. SYNCHRONVERTER

Synchronverter mimics the inertia physical characteristics of synchronous machine by using swing equation:

$$\frac{d\omega_s}{dt} = \frac{1}{J}(T_m - T_{ef} + D_p(\omega_r - \omega_s)) \tag{1}$$

$$\frac{d\delta_s}{dt} = \omega_s \tag{2}$$

where J is moment of inertia. T_m is a mechanical torque $T_m = P_{sref}/\omega_r$; D_p signifies a damping and drooping coefficient for the active power loop. ω_s is a virtual speed of synchronverter and ω_r is a reference system frequency. T_{ef} is electric torque, which is filtered output of T_e, and evaluated as,

$$T_e = \frac{3}{2}\psi_{ff} i_{sd} \tag{3}$$

where, i_{sd} is d component output current of VSC in dq frame. The ψ_{ff} is the filtered output of excitation flux ψ_f. It is obtained from the synchronverter reactive power loop given as:

$$\frac{d\psi_f}{dt} = \frac{1}{K}(Q_{sref} - Q_{sf} + D_q(V_{ref} - V_m)) \tag{4}$$

The bandwidth of this loop is controlled by K. K also represents the inertia of the reactive power loop. D_q is a voltage drooping coefficient which is kept as zero for operating in reactive power loop control. V_m is a peak value of sense voltage and V_{ref} and Q_{sref} are the reference values of V_m and reactive power Q_s respectively. The reactive power loop controls the ψ_f to regulate Q_s. Q_s is evaluated as:

$$Q_s = -\frac{3}{2}\omega_s \psi_{ff} i_{sq} \tag{5}$$

where, i_{sq} is q component output current of VSC in dq frame. Then voltage reference $e_s$of VSC is generated by synchronverter is expressed as:

$$e_s = \omega_s \psi_{ff} \tag{6}$$

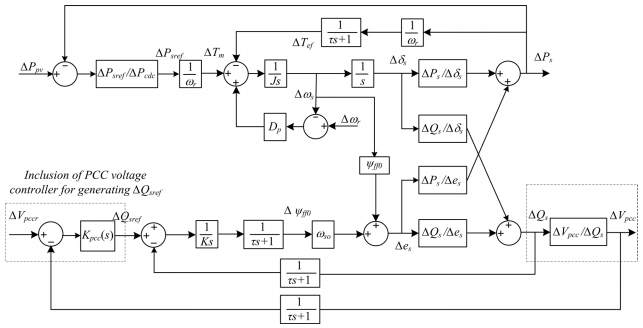

FIGURE 2. Block diagram of small-signal Model.

The above equations (1)-(6) are linearized around the operating point and a small-signal equations are obtained, where Δ represents a small perturbation. The small-signal equation of synchronverter are as follows:

$$s\Delta\omega_s = \frac{1}{J}\left(\frac{\Delta P_{sref}}{\omega_r} - \frac{\Delta P_s}{\omega_r} - D_p(\Delta\omega_s - \Delta\omega_r)\right) \tag{7}$$

$$s\Delta\delta_s = \omega_s \tag{8}$$

$$s\Delta\psi_f = \frac{1}{K}(\Delta Q_{sref} - \Delta Q_{sf} + D_q(\Delta V_{ref} - \Delta V_m) \tag{9}$$

$$\Delta e_s = \psi_{ffo}\omega_s + \omega_{so}\Delta\psi_{ff} \tag{10}$$

The active and reactive power loop of the synchronverter as a part of small-signal model diagram of the system, is as shown in Fig. 2 [22]. The $\Delta P_s/\Delta\delta_s$ and $\Delta Q_s/\Delta\delta_s$ are the transfer functions from small-signal angle change to active and reactive power, respectively. $\Delta P_s/\Delta e_s$ and $\Delta Q_s/\Delta e_s$ are the transfer functions of change in synchronverter emf to active and reactive power. The other blocks of Fig. 2 are discussed in the next subsections.

B. DC-LINK VOLTAGE CONTROLLER

The dc-link voltage controller makes sure that V_{dc} is regulated at the reference value V_{dcr} to deliver the desired active power from VSC to the grid, which is regulated by the following equation:

$$\frac{1}{2}C_{dc}\frac{dV_{dc}^2}{dt} = P_{pv} - P_s \tag{11}$$

From 11, it is noticed that V_{dc} is controlled by controlling output power of inverter P_s. The PV power supply to grid is:

$$P_{pv} = P_{cdc} + P_{loss} + P_s \tag{12}$$

where, P_{pv} is the PV array output power, P_{cdc} is power absorbed/supplied by the dc-link capacitor, P_{loss} is power loss in the VSC. In the equation 12, P_{cdc} and P_{loss} are almost negligible. Hence, P_{pv} can be control using P_s and can be used as control input in a dc-link controller.

$$P_{sref} = P_{pv} + K_v(V_{dcr}^2 - V_{dc}^2) \tag{13}$$

The V_{dc} fluctuates because of the difference between P_s and PV power P_{pv}. The power provided by the PV is controlled by V_{dc}. The compensator $K_v(s)$ controls the V_{dc} by

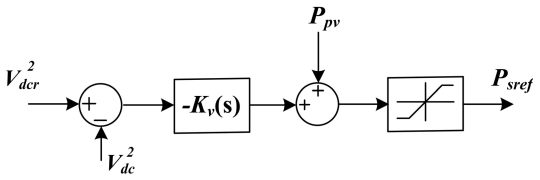

FIGURE 3. Control block diagram of dc-link voltage controller.

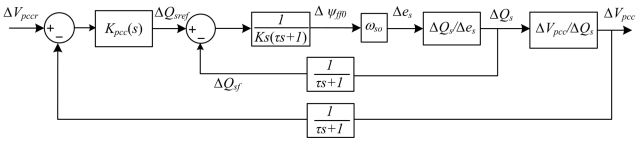

FIGURE 4. Simplified small-signal model of the proposed PV-STATCOM in PCC voltage control mode.

generating the P_{sref} for the active power loop. The $K_v(s)$ is given below in the equation (14) [28]. The dc-link voltage controller block diagram is shown in Fig. 3. The details of the controller design are discussed in section IV.

$$K_v(s) = \frac{1}{s}\beta_1 \frac{(s+\frac{\beta_2}{\beta_3})^2}{(s+\beta_2)^2} \tag{14}$$

where, β_1, β_2 and β_3 are the parameters of controller.

By linearizing the equation (11), $\Delta V_{dc}/\Delta P_{cdc}$ is obtained. The equation (13) is linearized to obtain $\Delta P_{sref}/\Delta V_{dc}$. The product of these two transfer functions $\Delta V_{dc}/\Delta P_{cdc}$ and $\Delta P_{sref}/\Delta V_{dc}$, $\Delta P_{sref}/\Delta P_{cdc}$ can be obtained.

$$\frac{\Delta P_{sref}}{\Delta P_{cdc}} = \frac{2}{sC_{dc}} K_v(s) \tag{15}$$

Active power loop of $\Delta P_s/\Delta P_{pv}$ as shown in Fig. 2. is completed by using $\Delta P_{sref}/\Delta P_{cdc}$.

C. PCC VOLTAGE CONTROLLER

Assuming that the $X_g \gg R_g$ and the grid impedance is mainly inductive. Hence, R_g can be considered as negligible and the PCC voltage amplitude V_{pcc} is given as:

$$\hat{V}_{pcc} = \hat{V}_g + \frac{(Q_s - Q_L)X_g}{3\hat{V}_{pcc}} \tag{16}$$

where, $X_g = \omega_r L_g$, Q_s is the inverter output reactive power, and V_g is the amplitude of grid voltage. By linearizing the equation (17), and by ignoring the 2^{nd} order term, one gets:

$$\Delta V_{pcc} = \frac{X_g}{3(2V_{pcc} - V_g)} \Delta Q_s \tag{17}$$

In the proposed control scheme, the outer loop is the PCC voltage controller, which generates the reference Q_{sref} for the reactive power loop.

The simplified diagram of PCC voltage control is given in Fig. 4, which is a simplified diagram taken from Fig. 2. Where $\Delta V_{pcc}/\Delta Q_s$ given in 17.

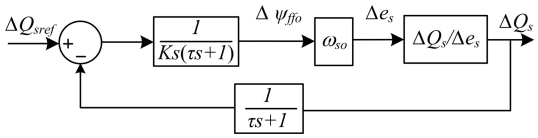

FIGURE 5. Simplified small-signal model of the proposed PV-STATCOM in reactive power control mode.

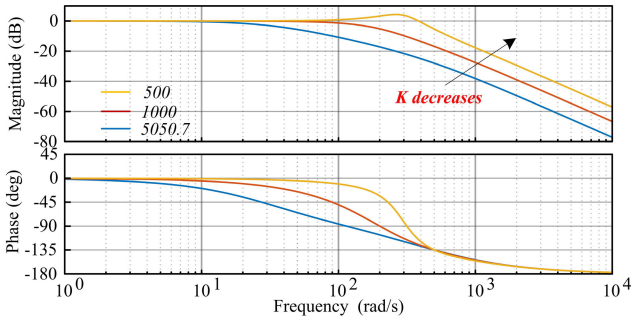

FIGURE 6. Bode Diagram of $H_{RPL}(s)$ with different K.

IV. CONTROLLER DESIGN

As described above, the PV system rating is 10.33 kW and the switching frequency of inverter is chosen as 10 kHz. The controllers are designed using the system ratings described in section II. The controllers are tuned using SISO tool in MATLAB/SIMULINK. Design for each of the controller is described in the following subsections.

A. SYNCHRONVERTER

In active power loop of synchronverter, D_p is a frequency droop coefficient which is selected based on the 100% change in real power for 0.25% change in system frequency. The frequency loop time constant τ_f, is chosen based on the amount of inertia provided by synchronverter. Larger the τ_f is larger the J, as given in equation 18. Here, τ_f is selected to be 0.01s.

$$J = \tau_f D_p \tag{18}$$

In reactive power loop, error between Q_{sref} and Q_s is fed to the integrator with gain $1/K$, which generates ψ_f. K decides the speed of response of reactive power loop. Assuming that the coupling effect from active power loop is weak, a simplified reactive power loop is obtained from Fig. 2, as shown in Fig. 5. The open loop gain of reactive power loop is:

$$H_{RPL} = \frac{\omega_{so}}{Ks(\tau_s + 1)} \frac{\Delta Q_s}{\Delta e_s} \tag{19}$$

The response of change in parameter K is observed in Fig. 6. As K decreases, bandwidth of the system increases with a decrease in phase margin. Further, for a lower value of K, overshoot is observed in bode plot. From the bode plot shown in Fig. 6, the K is chosen 5050.7.

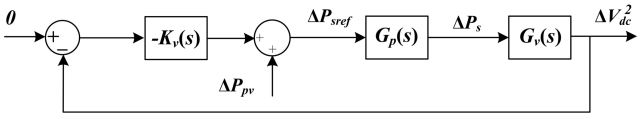

FIGURE 7. Control block diagram of designed of dc-link voltage controller.

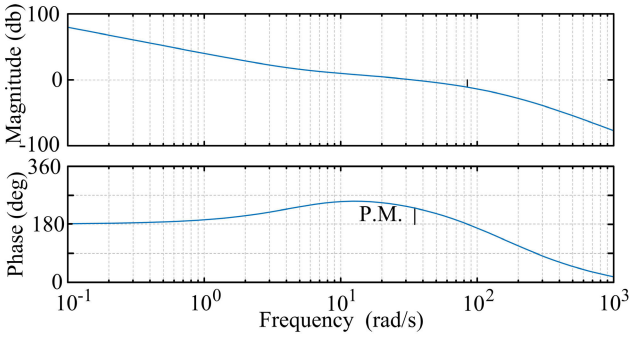

FIGURE 8. Bode plot of compensated dc-link voltage control loop.

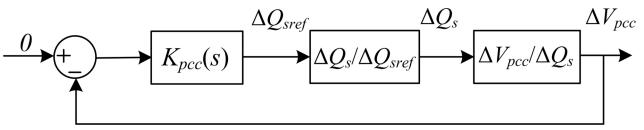

FIGURE 9. Control block diagram of PCC voltage control loop.

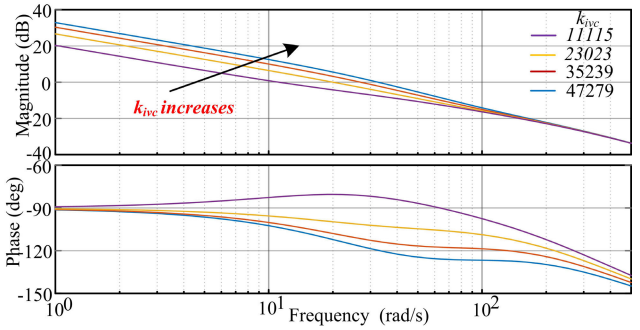

FIGURE 10. Bode Diagram of H_{vc} with different k_{ivc}.

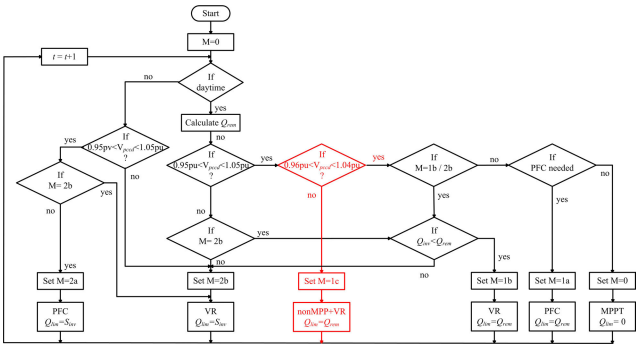

FIGURE 11. Flowchart of the proposed PV-STATCOM operating modes.

B. DC-LINK CONTROLLER DESIGN

Fig. 1 specifies that the error $V_{dcr} - V_{dc}$ is processed by compensator $K_v(s)$. The effect of P_{pv} is minimized by using it for feedforward compensation. The output of controller is P_{sref}, which is a active power reference for synchronverter. The $G_p(s)$ is a active power control transfer function, which is given as [22]:

$$G_p(s) = \frac{\Delta P_s}{\Delta P_{sref}} \tag{20}$$

The transfer function $G_v(s)$ reveals a relation between change of dc-link voltage V_{dc} with respect to P_s. $G_v(s)$ is obtained from solving and linearizing equation (11) as given in [28].

$$G_v(s) = \frac{\Delta V_{dc}^2}{\Delta P_s} = -\frac{2}{C_{dc}} \frac{\frac{2L_{eq}P_{pvo}}{3V_{sd}^2}s + 1}{s} \tag{21}$$

where, P_{pvo} is initial value of P_{pv} and L_{eq} is an equivalent inductance. Fig. 7 gives the open loop transfer function, which is as follows:

$$H_{dc}(s) = K_v(s)\frac{2}{C_{dc}} \frac{\frac{2L_{eq}(-P_{pvo})}{3V_{sd}^2}s + 1}{s} \frac{\Delta P_s}{\Delta P_{sref}} \tag{22}$$

The P_{pvo} is selected to be negative so that the controller is tune for the worst case as given in equation (22). The negative sign of $G_v(s)$ is compensate by multiplying $K_v(s)$ by -1.

The $K_v(s)$ contains an integrator to attain $V_{dcr} - V_{dc}$ to zero. Additionally, a gain is added in $K_v(s)$ to attain gain cross over frequency at 35 rad/sec. A lead compensator is added in $K_v(s)$ to stabilize the uncompensated loop with 50° phase margin. The bode plot with the compensated loop is shown in Fig. 8.

C. PCC VOLTAGE CONTROLLER DESIGN

The PCC voltage control block diagram is shown in Fig. 9. The PCC voltage controller open loop transfer function is as follows:

$$H_{vc}(s) = K_{pcc}s \frac{\omega_{so}(\tau_s + 1)(\Delta Q_s/\Delta e_s)}{Ks(\tau s + 1)(\tau s + 1) + \omega_{so}(\Delta Q_s/\Delta e_s)} \frac{\Delta V_{pcc}}{\Delta Q_s} \tag{23}$$

where,

$$K_{pcc}(s) = \frac{K_{pvc}s + k_{ivc}}{s} \tag{24}$$

The PI controller $K_{pcc}(s)$ is used to control PCC voltage. Fig. 10 shows the open loop bode plot of the PCC voltage controller. As the integrator parameter k_{ivc} increases, the speed of response of the system is increasing. As the PCC voltage loop is a outer loop which includes a reactive power loop as an inner loop. Therefore, the dynamics of the PCC voltage loop are slower than the reactive power loop. Hence, the PCC voltage controller is designed for phase margin 80° and cross over frequency 20 rad/s.

D. OPERATING MODE SELECTOR

Fig 11. shows the flow chart of the operation mode selector of PV-STATCOM which is inspired from [8]. Table 2

TABLE 2. PV-STATCOM operating modes.

Operating Modes		M
Partial STATCOM Mode	Power factor correction	1a
	Voltage Regulation	1b
	nonMPP+Voltage_regulation	1c
Full STATCOM Mode	Power factor correction	2a
	Voltage regulation	2b
Full PV Mode	-	0

gives the specific operating modes denoted by M. During the daytime, if insolation is less than the rated, then the remaining inverter capacity for reactive power Q_{rem} is calculated at every time step. In this case, if the PCC voltage is within a limit, power factor correction (PFC) mode may be activated to improve the system capacity by activating partial STATCOM mode (M=1a) of PV-STATCOM while limiting reactive power to Q_{rem}. The reactive power controller is selected in PFC mode. Due to disturbance, if the PCC voltage sags or swells, then voltage control mode is activated. If reactive power required to regulate the PCC voltage is less than Q_{rem}, then PV-STATCOM operates in a partial STATCOM mode (M=1b). If not, then the PV panels gets disconnect and the system operates in a Full STATCOM mode (M=2b). Once the PCC voltage gets regulated within the acceptable limit, the system mode changes manually to either of the following modes. The system changes to partial STATCOM Mode (M=1a) if PFC is required; otherwise, it operates in full PV mode (M=0). During the nighttime, the systems full capacity is utilized to exchange reactive power in both voltage control mode and reactive power control mode. If voltage fluctuates due to disturbance, the voltage control in full STATCOM mode is activated (M=2b). Once the voltage is regulated, the PFC control is activated in full STATCOM mode (M=2a).

During daytime, in case of a voltage drop, the PV system operating mode changes from MPP to non MPP mode (M=1c) instead of shifting to full STATCOM mode. Hence, due to reduction in the active power output of inverter, the Q_{rem} increases and the remaining capacity of inverter is used to recover voltage by injecting/absorbing reactive power. For this process, a limit is set (0.96 pu), so that it will alert the system before crossing the critical limit (0.95pu) and change the operating mode to non MPP mode and recover the voltage. In nonMPP mode if $Q_{inv} < Q_{rem}$, then the operating mode will be changed from partial PV-STATCOM mode (nonMPP) to full STATCOM mode.

V. SIMULATION RESULTS

Various operating modes of the proposed system are simulated in PSCAD/EMTDC software. A PV-STATCOM with conventional current controller [8] is taken for comparing performance of both the controllers. The main circuit parameters are taken same as the proposed system. For the conventional

TABLE 3. PV system parameters.

Parameter	Values	Parameter	Values
PV rated capacity	10 kW	J	0.40549 kg.m^2
V_{dc}	800 V	D_p	40.549 N.m.s/rad
C_{dc}	7000 μf	K	5050.7 Var.rad/V
Grid voltage(L-L)	0.4 kVrms	D_q	160.77 Var/V
Source voltage(L-L)	0.4 kVrms	K_{pvc}	552.552
R_f	0.2 Ω	K_{ivc}	23023
L_f	3.4 mH	β_1	1295.5
R_d	1 Ω	β_2	298
C_f	20 μf	β_3	55.5
R_t	304.98 Ω	τ	0.002 s
L_t	0.8 mH	Rated frequency	50 Hz

current control, the cut off frequency (ω_c) of the inner current control loop is taken as 1000 rad/sec. The dc-link control is designed for ω_c=100 rad/sec with phase margin of 80°. Cut off frequency ω_c and phase margin of the outer voltage control loop is 30 rad/sec and 88°, respectively. For synchronverter controller, the controller parameters are same as designed in the previous section. The system parameters for simulation studies are given in Table 3.

The simulation test is carried out in full STATCOM mode in daytime and at nighttime. Further, partial STATCOM mode with non-MPP and low voltage ride through tests are also carried out.

A. FULL STATCOM MODE- DAYTIME

In this case, initially system is operating in full PV mode. When PCC voltage goes below minimum limit, to regulate the voltage, the system control shifts to full STATCOM mode. The proposed PV-STATCOM is also compared with the conventional current control based PV-STATCOM in full STATCOM mode.

As shown in Fig. 12 for t <3 sec: The PV system is operating in MPP mode with available solar irradiation G=600 W/m^2. Active power (P_s) generated is 6 kW and the controller keeps the reactive power(Q_s) as near to zero since it is operating in a full PV mode. However, reactive power transfer of around 0.9 kVAR is observed which is supplied by a filter capacitor C_f. Initially, 2 kW active (P_L) and 2 kVAR reactive (Q_L) loads are connected to the system at PCC. Moreover, the grid supplies active power (P_g) and transfer reactive power (Q_g) to load. The PCC voltage (V_{pcc}) is 0.995 pu.

At t = 3 sec: A 2 kW and 6 kVAR large reactive load is connected at PCC and this leads to dropping of PCC voltage. When PCC voltage crosses the minimum limit, the full STATCOM mode is activated by virtually disconnecting the PV panel and the inverter starts injecting the reactive power in PCC and the PCC voltage is regulated within the defined limit. The requirement of entire load is fulfilled by the grid. A minimal amount of active power is absorbed by the DG system from the grid to compensate losses in it.

From Fig. 12(a), it can be observed that with conventional control, the undershoot in inverter frequency (f_s) is

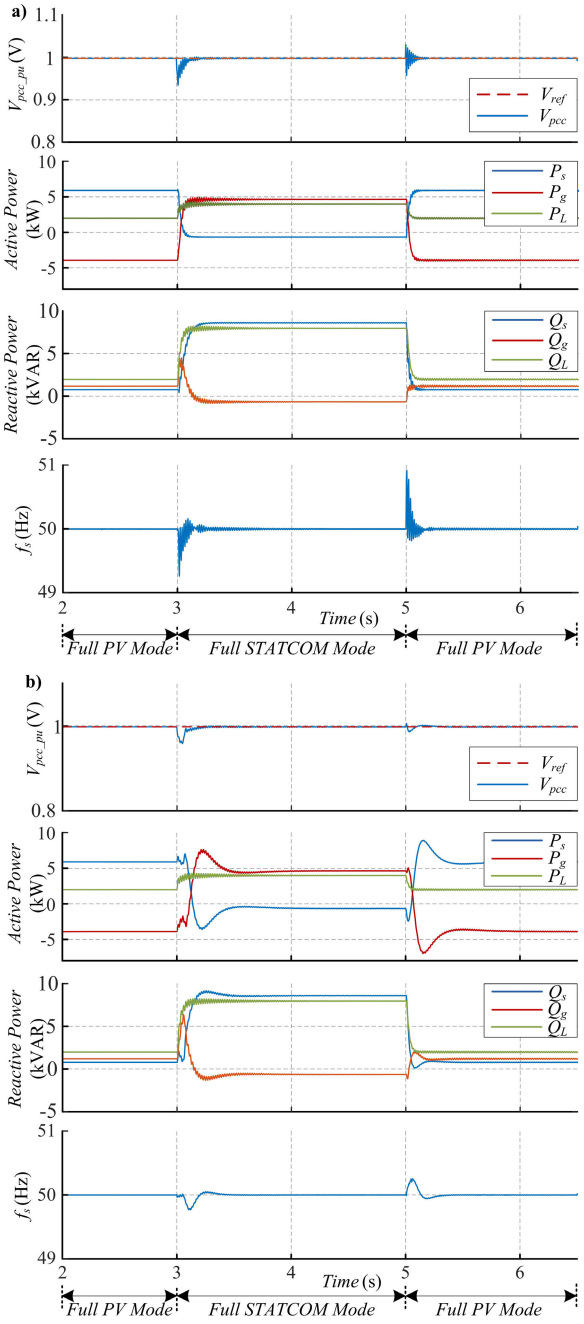

FIGURE 12. Simulation results for full STATCOM mode during daytime. (a) conventional PV-STATCOM (b) Proposed PV-STATCOM.

more for the same load change as compared to the proposed PV-STATCOM. The typical PV-STATCOM cannot provide inertia. The synchronverter based PV-STATCOM controls the frequency by providing the inertia from energy storage (here it is C_{dc}). When the load is added, the change in V_{pcc} is slower with synchronverter based PV-STATCOM controller. The speed of response of the proposed PV-STATCOM is slightly slower but comparable with typical PV-STATCOM.

At $t = 5$ sec: The extra-large load connected at PCC is removed and the controller again activates the full PV mode

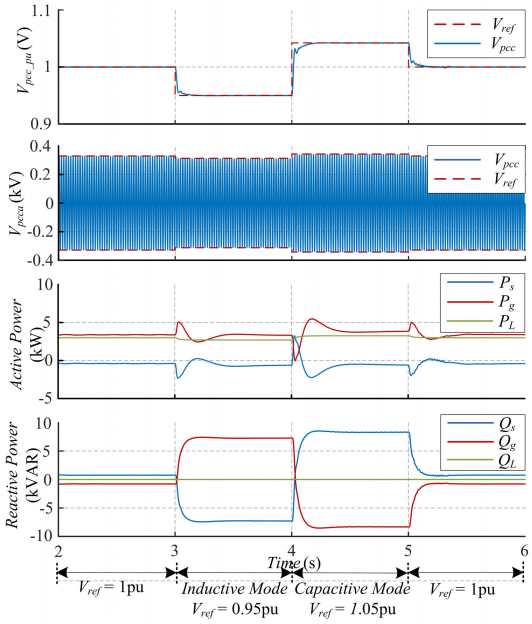

FIGURE 13. Simulation results for full STATCOM mode during nighttime of proposed PV-STATCOM.

by connecting the PV panel. As the V_{pcc} in the acceptable limit, the voltage control mode gets deactivated and sets reactive power reference to zero. DG starts supplying 6 kW active power and a small amount of reactive power exchange due to C_f. After supplying a minimal amount of Q_s to load, the remaining requirement of Q_L is fulfilled by the grid by supplying Q_g. It is also observed that the change in frequency is controlled due to inertia provided by the proposed system, which is not observed in the conventional control.

B. FULL STATCOM MODE- NIGHTTIME

This case validates the operation of the proposed system in full STATCOM mode at nighttime. The control purpose is to control PCC voltage and validate it in both the inductive and capacitive modes of operation, as shown in Fig. 13.

For $t < 3$ sec: The PV system is operating in full STATCOM mode. The PCC voltage reference is set to 1 pu. Initially, 3kW load is connected and is supplied by the grid as the solar insolation is zero.

At $t = 3$ sec: The V_{ref} changes from 1 pu to 0.95 pu. To follow the V_{ref}, the PCC voltage controller reduces the Q_{sref}, resulting in reactive power error less than zero. Due to negative error ψ_f decreases to reduce Q_s, so that it follows Q_{sref}. Hence, STATCOM changes its operation to inductive mode.

At $t = 4$ sec: The V_{ref} changes to 1.05 pu and STATCOM mode also changes from inductive to capacitive mode. As the V_{ref} increases, to regulate PCC voltage Q_{sref} also increases. This test proves the rapid performance of the proposed PV-STATCOM.

At $t = 5$ sec: The STATCOM gets back to its initial condition as V_{ref} changes to 1 pu. To regulate the voltage, Q_s gets reduce to its initial value.

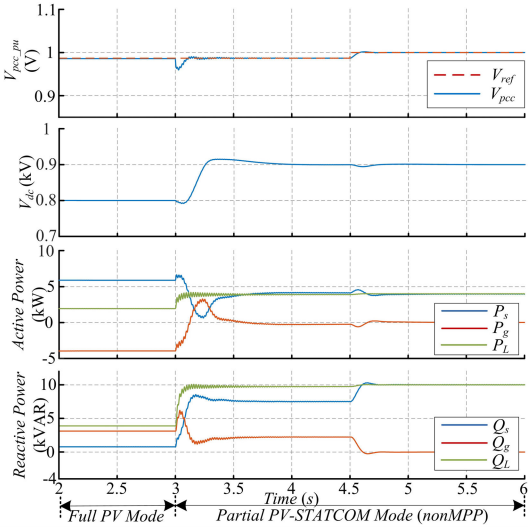

FIGURE 14. Simulation results for partial PV-STATCOM mode with nonMPP+voltage control.

C. PARTIAL PV-STATCOM MODE-nonMPP MODE

This case validates the partial PV-STATCOM mode when PV operates in a nonMPP mode. The control objective is to increase the Q_{rem} in critical conditions by shifting PV operating mode from MPP to nonMPP instead of shifting to Full STATCOM mode, as shown in Fig. 14.

For t <3 sec: Initially, PV system is operating in a Full PV MPP mode with G=600W/m^2 and $Q_{sref} = 0$ kVAR. The load connected at PCC is 2 kW and 4 kVAR.

At $t = 3$ sec: A 2 kW and 6 kVAR load are added at PCC and then the PCC voltage drops and goes below the limit of 0.96 pu. To avoid a voltage drop below the critical limit, Q_{rem} increases by changing PV operation to non MPP mode. As the G cannot be changed, V_{dcr} is changed to 900 V and voltage regains to its previous value i.e. 0.986 pu, by activating a voltage regulation mode as shown in Fig. 14. Due to reduction in active power injection from PV, more active power is supplied from the grid to load, which increases voltage drop at PCC. But due to nonMPP mode, share for reactive power increases and the extra voltage drop which occur due to nonMPP mode is recovered by injecting a minimal amount of reactive power to PCC.

At $t = 4.5$ sec: For regulating the PCC voltage at rated value, V_{ref} is changed to 1pu and V_{pcc} follows the reference as shown in Fig. 14. During this process, VSI injects more active power where Q_{rem} is almost equal to Q_{lim}.

D. LOW VOLTAGE RIDE THROUGH TEST - DAYTIME

As per the IEEE 1547 standard for voltage dip from 0.88 pu to 0.7 pu, the DG system should be operate under this condition for minimum time, which is defined a Low Voltage Ride Through (LVRT) are shown in Fig. 15(a). The test is performed when PV-system is in full PV mode. Initially, the output power of the DG is 8 kW and reactive power is set to zero. A large load is connected at PCC for 1.5 sec duration

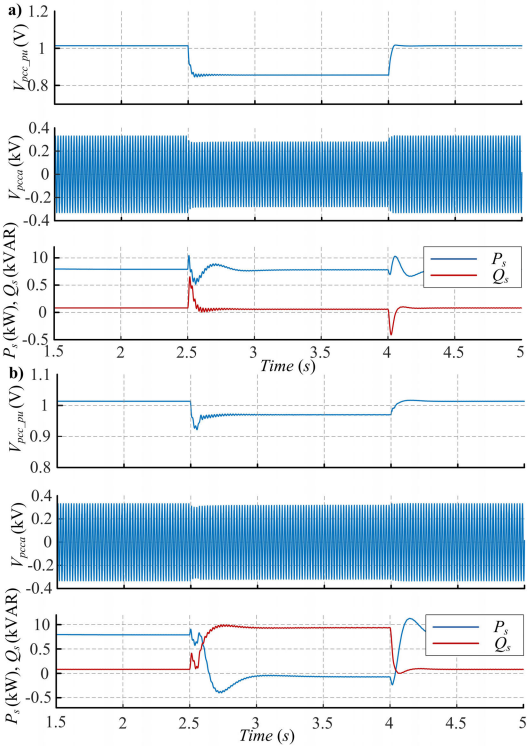

FIGURE 15. Simulation results for LVRT test (a) without PCC voltage control (b)With PCC voltage control.

at $t = 2.5$sec. At $t = 4$ sec, the large load connected is removed and the PCC voltage returns to its initial value. From Fig. 15(a), it is observed that the proposed PV-STATCOM complies the LVRT operation standard. After a disturbance, DG stays connected to the grid and continuously transfer 8 kW of real power.

As per IEEE 1547 standard the reactive power compensation is non-compulsory during LVRT. The performance of the proposed PV-STATCOM during LVRT is depicted in Fig. 15(b). Initially, condition for the LVRT test is same as previous test.

At $t = 2.5$ sec: A large load is connected at PCC. Due to this, grid start supplying Q_g to load as the PV operating in full PV mode. Due to this, PCC voltage dips and without a reactive compensator, PCC voltage becomes lesser than 0.88 pu. Whenever it goes below the lower limit of voltage limit, controller changes to a full STATCOM mode and solar panel are virtually disconnected from the system. The V_{pcc} brings the voltage reference to 0.97 pu and full capacity of theVSC is used to control V_{pcc} i.e. reactive power Q_s supplied by the inverter is 10 kVAR. If voltage reference is more than 0.97 pu, more reactive power needs to be supplied from the inverter, and it crosses the inverter capacity.

At $t = 4$ sec: PV system returns to full PV mode after removing the large load. PV panel connects to inverter and started supplying active power 8 kW. Q_{sref} is set to zero and a minimal amount of Q_s is supplied from inverter due to filter capacitor C_f.

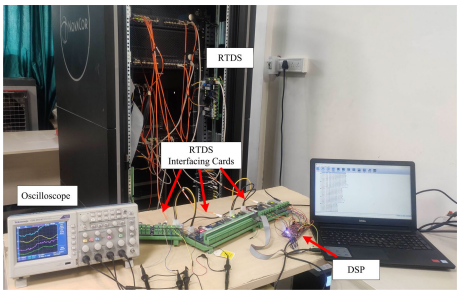

FIGURE 16. CHIL implementation setup.

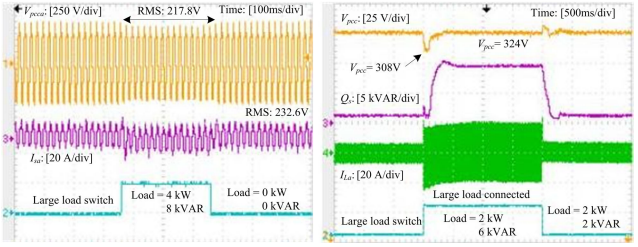

FIGURE 17. CHIL results (a) Full PV mode (b) proposed PV inverter operation in full STATCOM mode.

This test validates that the proposed smart inverter operation sustains during LVRT operation as per IEEE 1547 standard, and successfully regulates the voltage while providing reactive power compensation.

VI. CHIL RESULTS

Several experiments are performed with CHIL. The same system is considered for this test as in the simulation test. The simulation results are carried out with RTDS. The sensed voltage and current signal are sent to TMS320F28377s microcontroller through ADC channel. The controller is implemented in DSP based unit TMS320F28377s; which generates the firing pulses to switch inverter based on objectives and sent through DAC channel to RTDS. The experimental setup is shown in Fig.16.

A. FULL STATCOM MODE

The effect of a large load connected to the PV system is shown in Fig.17(a). Initially, no load is connected and real power transfer by the system is 5 kW. As soon as the load is connected, the PCC voltage drops from1.01 pu to 0.94 pu (232.6 V to 217.8 V). When the load is removed PCC, voltage returns to the initial value i.e. to 1.01 pu.

Fig 17(b) shows the test results in full STATCOM mode. Initially, the system is operating in full PV mode and load connected at PCC is 2kW, 2kVAR. The real power generated by PV is 5 kW. The reactive power exchange is set to zero, but DG supplies a minimal amount of reactive power due to the presence of C_f as shown in Fig. 17(b). When the large load of 2 kW, 6kVAR is connected, the voltage dip at PCC is observed. The PV panel is disconnected, and the system shifts to full STATCOM mode. The PCC voltage

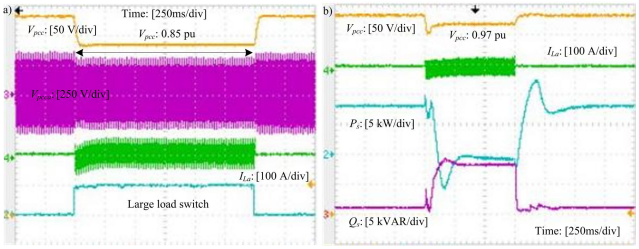

FIGURE 18. CHIL results for LVRT test (a) without PCC voltage control (b)With PCC voltage control.

controller is activated, and the voltage is regulated at a initial value. The load current (I_{La}) is reduced when a large load is disconnected, and the system shifts to full PV mode. PCC voltage controller is deactivated as there is no need for voltage regulation.

B. LVRT TEST

Fig 18(a) shows the LVRT test carried during full PV mode and depicted the V_{pcc} in pu, PCC voltage of a phase (V_{pcca}), load current (I_{La}) and load switch. Initially, the PV system generates 8 kW power and Q_{sref} is set to zero; the load is not connected at PCC, so reverse power flow in the grid increases the PCC voltage to 1.01pu. A large load is connected at PCC and PV and the grid starts supplying power to load, which causes dip in PCC voltage to 0.84 pu. The load is disconnected after 1.5 sec and after that, PCC voltage again increases to 1.01 pu. When the load is connected, the PV system stays connected and rides through the entire period. Hence, it successfully fulfills the criterion of the IEEE 1547 Standard for LVRT.

The LVRT test with a reactive power compensation is shown in Fig 18 (b), which depicts the PCC voltage of a phase (V_{pcca}), PV active power (P_s), DG system reactive power (Q_s), and load current (I_{La}). Initially, the power generated by PV is 8 kW and the load connected at PCC is 2 kW and 2 kVAR. PV system operating in full PV mode, so ideally reactive power exchange with the grid is zero; however, filter capacitor C_f supply 0.8 kVAR reactive power. When a large load is connected, the controller detects a drop in PCC voltage at turn-on Full STATCOM mode. The real power generated by PV is set zero by increasing voltage across PV panel. The PCC voltage is regulated at 0.97 pu and for that, the inverter supplies 9 kVAR reactive power. After 1.5 sec, a load is removed and the system again shifts to full PV mode. As there is no need to regulate PCC voltage, the reactive power reference is zero. This test validates the proposed PV-STATCOM during LVRT with reactive power compensation and completes the IEEE 1547 standard requirement.

C. CHANGE OF SHORT CIRCUIT RATIO (SCR)

This test is carried out to validate and compare performance of the proposed PV-STATCOM with conventional PV-STATCOM with a change in short circuit ratio (SCR). As the grid impedance increases, SCR of the system

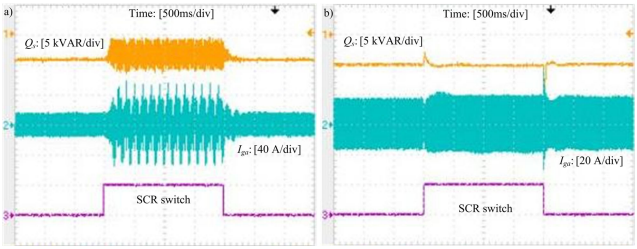

FIGURE 19. CHIL results with reactive power control (a) conventional PV-STATCOM (b) proposed PV-STATCOM.

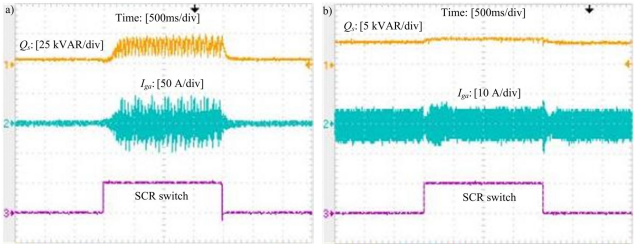

FIGURE 20. CHIL results with PCC voltage control (a) conventional PV-STATCOM (b) proposed PV-STATCOM.

decreases and vice versa. So, change in SCR affects the grid stiffness.

Initially, the PV system is functioning in partial STATCOM mode and reactive power control is activated. PV generate 5kW real power and exchange reactive 5 kVAR reactive power in inductive mode. At $t = 3$ sec, SCR of the grid adjusted from 4.4 to 2.7. It is observed from Fig. 19, that the response of Q_g and Q_s is oscillatory with a conventional PV-STATCOM, but it is quite stable with the proposed PV-STATCOM.

Fig. 20 shows the change in SCR response during voltage control mode of proposed and typical PV-STATCOM. The system is operating in partial STATCOM mode with 5 KW real power generation and 2 kW, 2 kVAR load connected at PCC. The voltage controller regulates PCC voltage to 1pu by supplying 4 kVAR reactive power Q_s. When SCR changes from 4.4 to 2.7, the proposed STATCOM gives a stable response shown in Fig 20(b), with an increased injection of reactive power to regulate voltage. Also, the response of grid current is quite stable at lower SCR. When SCR again changes from 2.7 to 4.4 proposed STATCOM restores the previous values. However, the response is different for typical current control. With reduce SCR, the grid current and system parameter response is oscillatory as shown in Fig. 20(a).

Therefore, it can be said that performance of the proposed PV-STATCOM is better than typical PV-STATCOM under weak grid conditions in both reactive power control and voltage control mode.

VII. CONCLUSION

This paper proposes the synchronverter based PV-STATCOM. The synchronverter mimics the synchronous machines and its primary function is to reduce the frequency deviation by providing inertia and in the same manner, the synchronverter can also be used for reactive power compensation. The efficacy of the proposed PV-STATCOM is checked with 10 kVA PV plant during night and day at different operating modes. The performance is validated on PSCAD/EMTDC software-based simulation study and CHIL with RTDS and microcontroller. The following conclusions can be drawn:

1) The proposed PV-STATCOM is validated at different operating modes. In partial STATCOM mode, it can successfully use the remaining capacity of inverter for reactive power compensation. In full STATCOM mode, it successfully operates as STATCOM. Also, the frequency control is achieved as it is inherently present in synchronverter. The proposed system provides a fast and flexible response for both frequency and PCC voltage control.
2) An additional nonMPP operating mode increases the systems reactive power capability and successfully controls the system voltage by adjusting the active power generation.
3) The LVRT test performed on the proposed PV-STATCOM demonstrates that it meets the LVRT requirement of IEEE 1547 standard. Also, it regulates the PCC voltage during LVRT by providing reactive power compensation. The system is stable during LVRT as a PV-STATCOM.
4) Due to impedance interaction between the PV system and grid, in both reactive power and voltage control mode, the proposed PV-STATCOM performs in more stable manner in both the controller mode.
5) The proposed controller may allow parallel operation of inverters with voltage control by using PCC voltage control plus voltage droop control mode, which can be a topic of further study.

REFERENCES

[1] E. L. da Silva, J. J. Hedgecock, J. C. O. Mello, and J. C. F. da Luz, "Practical cost-based approach for the voltage ancillary service," *IEEE Trans. Power Syst.*, vol. 16, no. 4, pp. 806–812, Nov. 2001.
[2] N. G. Hingorani, L. Gyugyi, and M. El-Hawary, *Understanding FACTS: Concepts and Technology of Flexible AC Transmission Systems*, vol. 1. New York, NY, USA: IEEE Press, 2000.
[3] R. K. Varma and V. Khadkikar, "Utilization of solar farm inverter as STATCOM," U.S. Patent 2016/0 197 482 A1, Sep. 15, 2009.
[4] R. K. Varma, *Smart Solar PV Inverters with Advanced Grid Support Functionalities*. Hoboken, NJ, USA: Wiley, 2021.
[5] R. K. Varma, V. Khadkikar, and R. Seethapathy, "Nighttime application of PV solar farm as STATCOM to regulate grid voltage," *IEEE Trans. Energy Convers.*, vol. 24, no. 4, pp. 983–985, Dec. 2009.
[6] R. K. Varma, S. A. Rahman, A. C. Mahendra, R. Seethapathy, and T. Vanderheide, "Novel nighttime application of PV solar farms as STATCOM (PV-STATCOM)," in *Proc. IEEE Power Energy Soc. Gen. Meeting*, Jul. 2012, pp. 1–8.
[7] R. K. Varma, S. A. Rahman, and T. Vanderheide, "New control of PV solar farm as STATCOM (PV-STATCOM) for increasing grid power transmission limits during night and day," *IEEE Trans. Power Del.*, vol. 30, no. 2, pp. 755–763, Apr. 2015.
[8] R. K. Varma and E. M. Siavashi, "PV-STATCOM: A new smart inverter for voltage control in distribution systems," *IEEE Trans. Sustain. Energy*, vol. 9, no. 4, pp. 1681–1691, Oct. 2018.
[9] R. K. Varma, E. M. Siavashi, S. Mohan, and T. Vanderheide, "First in Canada, night and day field demonstration of a new photovoltaic solar-based flexible AC transmission system (FACTS) device PV-STATCOM for stabilizing critical induction motor," *IEEE Access*, vol. 7, pp. 149479–149492, 2019.

[10] R. K. Varma and M. Akbari, "Simultaneous fast frequency control and power oscillation damping by utilizing PV solar system as PV-STATCOM," *IEEE Trans. Sustain. Energy*, vol. 11, no. 1, pp. 415–425, Jan. 2020.
[11] R. A. Walling and K. Clark, "Grid support functions implemented in utility-scale PV systems," in *Proc. IEEE PES T&D*, Mar. 2010, pp. 1–5.
[12] F. L. Albuquerque, A. J. Moraes, G. C. Guimarães, S. M. R. Sanhueza, and A. R. Vaz, "Photovoltaic solar system connected to the electric power grid operating as active power generator and reactive power compensator," *Sol. Energy*, vol. 84, no. 7, pp. 1310–1317, Jul. 2010.
[13] R. R. Mishra and P. Tripathi, "Recent developments in PV–static synchronous compensator," in *Proc. 2nd Int. Conf. Innov. Mech. Ind. Appl. (ICIMIA)*, Mar. 2020, pp. 658–664.
[14] Y. Zhao and B.-W. Sun, "Research on STATCOM principle and control technology," in *Proc. Int. Conf. Consum. Electron., Commun. Netw.*, Apr. 2011, pp. 1593–1596.
[15] S. Iyer, A. Ghosh, and A. Joshi, "Inverter topologies for DSTATCOM applications—A simulation study," *Electr. Power Syst. Res.*, vol. 75, nos. 2–3, pp. 161–170, 2005.
[16] B. Singh, K. Al-Haddad, R. Saha, and A. Chandra, "Static synchronous compensators (STATCOM): A review," *IET Power Electron.*, vol. 2, no. 4, pp. 297–324, Jul. 2009.
[17] S. B. Subramanian, S. Mohan, M. Akbari, H. Maleki, R. Salehi, W. H. Litzenberger, and R. K. Varma, "Control of STATCOMs—A review," in *Proc. IEEE Power Energy Soc. Gen. Meeting (PESGM)*, Aug. 2018, pp. 1–5.
[18] P.-L. Nguyen, Q.-C. Zhong, F. Blaabjerg, and J. M. Guerrero, "Synchronverter-based operation of STATCOM to mimic synchronous condensers," in *Proc. 7th IEEE Conf. Ind. Electron. Appl. (ICIEA)*, Jul. 2012, pp. 942–947.
[19] L. do N. Gomes, A. J. G. Abrantes-Ferreira, R. F. da S. Dias, and L. G. B. Rolim, "Synchronverter-based STATCOM with voltage imbalance compensation functionality," *IEEE Trans. Ind. Electron.*, vol. 69, no. 5, pp. 4836–4844, May 2022.
[20] L. Vetoshkin and Z. Müller, "Dynamic stability improvement of power system by means of STATCOM with virtual inertia," *IEEE Access*, vol. 9, pp. 116105–116114, 2021.
[21] Q.-C. Zhong and G. Weiss, "Synchronverters: Inverters that mimic synchronous generators," *IEEE Trans. Ind. Electron.*, vol. 58, no. 4, pp. 1259–1267, Apr. 2011.
[22] A. Sonawane and A. Umarikar, "Small-signal stability analysis of PV-based synchronverter including PV operating modes and DC-link voltage controller," *IEEE Trans. Ind. Electron.*, vol. 69, no. 8, pp. 8028–8039, Aug. 2022.
[23] A. J. Sonawane and A. C. Umarikar, "Three-phase single-stage photovoltaic system with synchronverter control: Power system simulation studies," *IEEE Access*, vol. 10, pp. 23408–23424, 2022.
[24] G. Li, F. Ma, Y. Wang, M. Weng, Z. Chen, and X. Li, "Design and operation analysis of virtual synchronous compensator," *IEEE J. Emerg. Sel. Topics Power Electron.*, vol. 8, no. 4, pp. 3835–3845, Dec. 2020.
[25] C. Li, R. Burgos, I. Cvetkovic, D. Boroyevich, L. Mili, and P. Rodriguez, "Analysis and design of virtual synchronous machine based STATCOM controller," in *Proc. IEEE 15th Workshop Control Modeling Power Electron. (COMPEL)*, Jun. 2014, pp. 1–6.
[26] S. Yazdani, M. Ferdowsi, and P. Shamsi, "Virtual inertia based control of PV-STATCOM: Operation under unbalanced frequency and grid conditions," in *Proc. IEEE Kansas Power Energy Conf. (KPEC)*, Jul. 2020, pp. 1–4.
[27] K. H. Hussein, I. Muta, T. Hoshino, and M. Osakada, "Maximum photovoltaic power tracking: An algorithm for rapidly changing atmospheric conditions," *IEE Proc.-Generat., Transmiss. Distrib.*, vol. 142, no. 1, pp. 59–64, Jan. 1995.
[28] A. Yazdani and R. Iravani, *Voltage-Sourced Converters in Power Systems: Modeling, Control, and Applications*. Hoboken, NJ, USA: Wiley, 2010.

AJINKYA J. SONAWANE (Student Member, IEEE) was born in Maharashtra, India. He received the B.E. degree in electrical engineering from Pune University, Maharashtra, in 2012, and the M.Tech. degree in integrated power systems from the Yeshwantrao Chavan College of Engineering, Nagpur, India, in 2015. He is currently pursuing the Ph.D. degree with the Department of Electrical Engineering, Indian Institute of Technology at Indore, Indore, India.

His current research interest includes renewable energy generation systems.

AMOD C. UMARIKAR (Member, IEEE) was born in Maharashtra, India. He received the M.Tech. degree in power electronics and power systems from the Indian Institute of Technology Bombay, Mumbai, India, in 2000, and the Ph.D. degree in electrical engineering from the Indian Institute of Science, Bengaluru, India, in 2006.

He is currently a Professor with the Department of Electrical Engineering, Indian Institute of Technology at Indore, Indore, India. His current research interests include the application of power electronics in renewable energy systems and power quality.